John von Neumann Institute for Computing

Silicon Surfaces Functionalized with Organic Molecules: Uracil Adsorption as a Prototypical Example

Wolf G. Schmidt, Kaori Seino, Martin Preuss,
Patrick H. Hahn, Friedhelm Bechstedt

published in

NIC Symposium 2004, Proceedings,
Dietrich Wolf, Gernot Münster, Manfred Kremer (Editors),
John von Neumann Institute for Computing, Jülich,
NIC Series, Vol. **20**, ISBN 3-00-012372-5, pp. 205-214, 2003.

http://www.fz-juelich.de/nic-series/volume20

Silicon Surfaces Functionalized with Organic Molecules: Uracil Adsorption as a Prototypical Example

Wolf G. Schmidt, Kaori Seino, Martin Preuss, Patrick H. Hahn, and Friedhelm Bechstedt

Computational Materials Science Group
Institut für Festkörpertheorie und Theoretische Optik
Friedrich-Schiller-Universität Jena
Max-Wien-Platz 1, 07743 Jena, Germany
E-mail: {wgs, seino, preuss, patrick, bechsted}@ifto.physik.uni-jena.de

The structural, electronic and optical properties of the uracil-covered Si(001) surface have been studied by DFT-GGA calculations. Dative-bonded configurations are characterized by a high density of surfaces states in the energy region of the fundamental gap, whereas the surface is perfectly passivated when covalent bonds form between the molecule and the substrate. A remarkable influence of the adsorption configuration on the surface optical properties is predicted. The results show that semiconductor surface properties can be tuned within a very wide range by organic functionalization even with only one molecular species.

1 Introduction

As discussed in the following section, there is currently great interest in producing and characterizing organically modified semiconductor surfaces. Using grants of Cray T3E time provided by the John von Neumann Institut for Computing (NIC), we have investigated the reaction mechanisms, interface geometries, electronic properties and optical spectra of a variety of organic/inorganic interfaces. In detail, we studied the adsorption of pyrrole and polypyrrole[1], cyclopentene[2], methylchloride[3], and uracil[4] on the Si(001) surface. The latter system can be considered as a prototypical example for the interaction of small organic molecules with a semiconductor surface. Our main results on uracil covered Si(001) surface are discussed in this report.

2 Motivation

The (001) surface of silicon is the starting point for the fabrication of most microelectronic devices. Therefore, Si surface reactions with metals, hydrogen, oxygen and halogens have been intensively studied in the past[5]. However, in recent years there is an increasing interest in developing methods for coupling microelectronics with organic-based structures for applications such as nonlinear optics, thin-film displays, lithography, and molecular electronics. For this reason, much effort has been devoted to the preparation and characterization of ultra-thin organic layers on Si(001) surfaces. Organic overlayers may also facilitate the attachment of biomolecules, such as DNA, to the semiconductor surface.

Much progress has been made in recent years in understanding the reactions of simple unsaturated organic molecules with the Si(001) surface. Alkenes, for example, can react with Si dimers via a $[2 + 2]$ cycloaddition reaction and may thus form very well ordered

organic films[6–8]. Potentially more interesting are surface reactions with polyfunctional organic molecules. They may allow for creating an ordered array of possible further reaction sites, provided the functional groups remain intact. However, the interaction of polyfunctional organic molecules with semiconductor surfaces is often poorly understood, because of the many surface reactions possible. Molecules containing two conjugated double bonds may react with the Si(001) surface via $[4+2]$ Diels-Alder reactions[9] as well as via $[2+2]$ cycloadditions. A large variety of interface structures may form for heterocyclic amines, which in addition to C=C double bonds also contain N-H bonds. The configuration formed via N-H bond cleavage is favorable in the case of pyrrole, for example[10–12, 1]. $[2+2]$ C=O cycloaddition reactions as well as α-hydrogen transfers to Si dangling bonds are discussed for the adsorption of ketones on Si(001)[13–16].

In the present study we investigate as a model case the chemisorption of uracil on the Si(001) surface. This system was previously investigated with scanning tunneling microscopy (STM) and high-resolution electron energy-loss spectroscopy (HREELS)[17]. The STM images show that uracil may form ordered overlayer structures. The HREELS spectra yield a stronger intensity of the in-plane modes compared with the out-of-plane vibrations, indicating that the orientation of the molecular plane is upright. Some uracil:Si(001) bonding configurations were also already probed computationally, using an eight-atom cluster to model the Si surface[17]. Uracil contains one C=C double bond, two N-H bonds, and two carbonyl bonds (C=O). Therefore, surface reaction scenarios similar to the ones discussed above for alkenes, amines or ketones may occur and are investigated in the present study using *first-principles* calculations.

3 Method

The total-energy and electronic-structure calculations are performed using the Vienna Ab-initio Simulation Package (VASP) implementation[18] of the gradient-corrected[19] density functional theory (DFT-GGA). The electron-ion interaction is described by non-normconserving ultrasoft pseudopotentials[20, 21], allowing for the accurate quantum-mechanical treatment of first-row elements with a relatively small basis set of plane waves. We expand the electronic wavefunctions into plane waves up to an energy cutoff of 25 Ry, which has been demonstrated to be sufficient in our study on DNA base molecules[22].

The Si(001) surface is modeled with a periodically repeated slab. The supercell consists of 8 atomic Si layers plus adsorbed molecules and a vacuum region equivalent in thickness to 12 atomic layers. The Si bottom layer is hydrogen saturated and kept frozen during the structure optimization. The topmost 5 layers of the slab as well as the adsorbed molecules are allowed to relax.

The residual minimization method – direct inversion in the iterative subspace (RMM-DIIS) algorithm[23, 24, 18] is employed to minimize the total energy of the system. The surface structure is considered to be in equilibrium when the Hellmann-Feynman forces are smaller than 10 meV/Å. The Brillouin zone integrations are performed using sets corresponding to 64 **k** points in the full (1×1) surface Brillouin zone (SBZ).

Surface optical spectra are determined from all-electron wave functions obtained by the projector-augmented wave (PAW) method[25]. Transition matrix elements have been calculated for **k**-point sets corresponding to 256 points in the full SBZ. The slab polarizability is calculated in the independent-particle approximation. A scissors operator approach has

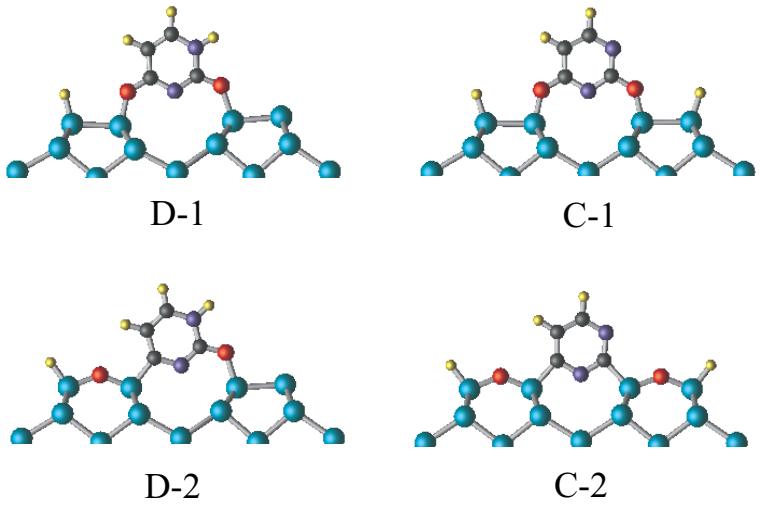

Figure 1. Uracil/Si(001) adsorption configurations. Grey, purple, blue, red, and yellow symbols indicate C, N, Si, O, and H atoms, respectively.

been used to account for the band-gap underestimation of 0.5 eV for bulk Si due to the neglect of self-energy effects within the DFT. Reflectance anisotropy spectra (RAS) have been calculated from the slab polarizability according to the scheme devised by Del Sole and co-workers[26,27].

The calculations are massively parallelized with respect to the electronic states, the plane-wave coeffizients, and **k** points using message passing interface (MPI). On the Cray T3E we observe a very good scaling behaviour using up to 64 processors.

4 Results

4.1 Main Adsorption Geometries

We investigated a very large number of plausible adsorption geometries and reaction paths for uracil adsorbed on Si(001)[4]. From these total-energy calculations in conjunction with experimental work[17] it can be concluded that uracil adsorption on Si(001) is likely to result in the dimer bridging configurations shown in Fig. 1. Starting from a dative-bonded configuration, where uracil is attached to the electron-poor "down" Si dimer atom via one carbonyl group, a relative low energy barrier of about 0.3 eV needs to be overcome for hydrogen dissociation, molecular rotation around the surface normal and tilting towards the neighboring Si dimer[4]. This leads to the configurations where uracil is partially dative (D-1 in Fig. 1) or completely covalently (C-1) bonded to the Si surface bridging two Si dimer rows, respectively. An energy barrier larger than one eV needs to be overcome for oxygen insertion into Si dimers, leading to the very favorable interface configurations D-2 and C-2[4]. The formation of these structures therefore requires annealing at elevated temperatures. The calculated adsorption energies of the models D-1, C-1, D-2, and C-2 amount to 2.77, 3.66, 3.78, and 5.27 eV, respectively. The dative bond in the structures

D-1 and D-2 occurs between the electron-rich uracil carbonyl group and the electron-poor atom of the clean Si dimer. It is about 0.1 Å longer than the corresponding covalent Si-O bond[4].

4.2 Uracil Induced Changes of the Si(001) Surface Electronic Properties

The surface band structures calculated for the structural models discussed above can be clear-cut classified. Models C-1 and C-2, where exclusively covalent bonds occur, lead to a perfect surface passivation, as shown for the latter case in Fig. 2. The Si-dimer related π and π^* bands characteristic for the clean Si(001) surface[5] disappear, due to the formation of Si-O and Si-C σ bonds, which lie energetically below the bulk Si valence band edge. The corresponding antibonding σ^* combinations occur above the Si conduction band edge. No molecular electronic states exist in the energy region of the Si fundamental gap. The highest occupied and lowest unoccupied molecule states, V_M and C_M, respectively, occur below and above the bulk valence and conduction band edges (cf. Fig. 2).

The situation is very different for the partially dative bonded models D-1 and D-2. We find two prominent surface states, S_1 and S_2, in the energy region of the Si bulk band gap (cf. Fig. 2). At least within DFT-GGA, which usually suffers from an underestimation of excitation energies[28], these two states give rise to a semimetallic band structure and pin the Fermi level. The orbital character of S_1, shown in Fig. 2, is very similar to the surface state localized at the "up" dimer atom of the clean Si(001) surface[5]. The dispersion of S_1 perpendicular to the dimer row direction is very small, whereas a large dispersion is calculated for the direction parallel to the dimer rows. The S_2 state is uracil derived. It is mainly formed by non-bonding carbon and nitrogen p orbitals. Again, due to the interaction between neighboring molecules, a strong dispersion for the direction parallel to the dimer rows is predicted. Thus, a one-dimensional conducting structure forms. The oxidation of the first Si layer (D-1 $\rightarrow$ D-2) decreases the energy separation between S_1 and S_2.

In order to investigate the variation of the surface dipole layer upon adsorption of uracil, the microscopic electrostatic potential calculated within DFT-GGA

$$V_C(\mathbf{r}) = V_{ps}^{local}(\mathbf{r}) + V_H(\mathbf{r}) \tag{1}$$

is considered[29]. Here $V_{ps}^{local}(\mathbf{r})$ is the local part of the pseudopotential and $V_H(\mathbf{r})$ is the Hartree potential. The averaged and smoothed electrostatic potential in [001] direction is given by

$$\overline{V_C}(z) = \frac{1}{L}\int_{z-L/2}^{z+L/2} dz' \frac{1}{A}\int_A dxdy V_C(x,y,z'), \tag{2}$$

where A is the area of the surface unit cell and L the distance between the substrate layers. In Fig. 3 the difference $\overline{\Delta V_C}(z)$ between the uracil/Si interface configurations and the clean relaxed Si(001)(4×2) surface is shown. It can be seen that the D-1 and D-2 bonding configurations of uracil on Si(001) lead to a drastic reduction of the Si(001) surface dipole potential by more than two eV. The change of the surface dipole potential equals the change in the ionization energy. After the formation of covalent bonds, i.e., for the structures C-1 and C-2, the surface dipole of the uracil/Si interface is rather close to the value of the clean surface.

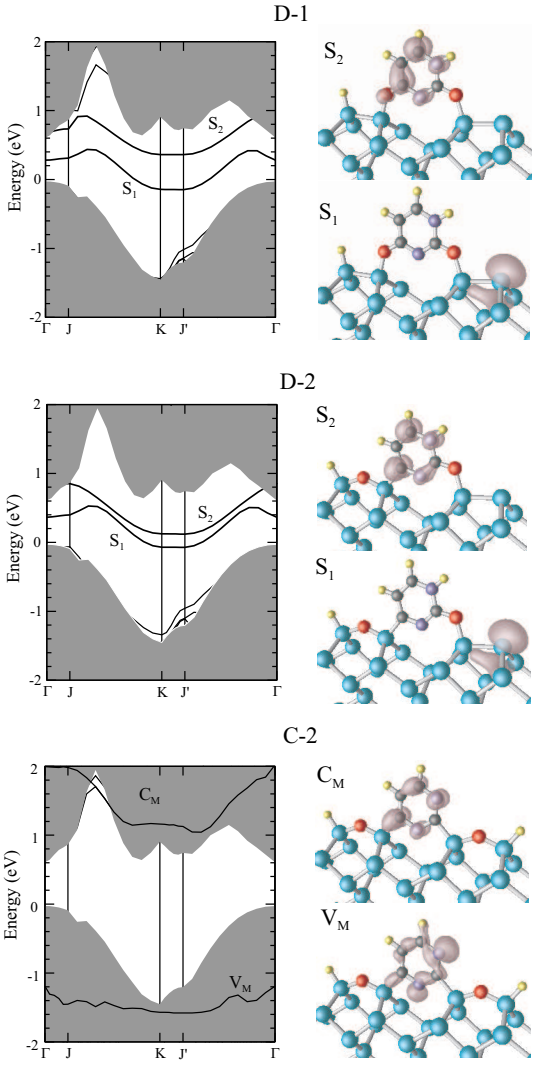

Figure 2. Surface band structures for the interface models D-1, D-2, and C-2 in Fig. 1. Grey regions indicate the projected Si bulk bands. In the right panel, the orbital character of specific states is indicated by isosurfaces for 0.05 Å^{-3}.

In order to explore the uracil induced changes of the electronic structure in more detail we compute the charge difference

$$\Delta\rho(\mathbf{r}) = \rho_{U/Si}(\mathbf{r}) - \rho_{Si}(\mathbf{r}) - \rho_{U}(\mathbf{r}), \tag{3}$$

where $\rho_{U/Si}$ is the (negative) electron density calculated for the slab describing the uracil adsorbed Si(001) surface, ρ_{Si} is that for the clean relaxed Si(001) surface and ρ_U is that for a gas-phase uracil molecule in the (possibly dissociated) configuration assumed for the respective bonding geometry. The positive and negative charge differences allow to

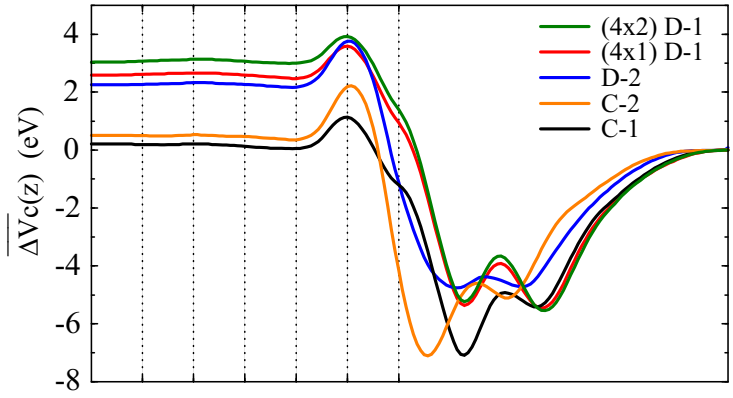

Figure 3. Difference of the averaged and smoothed electrostatic potentials of uracil:Si adsorption configurations and the clean Si(001) surface plotted along the surface normal in the interface region. Dashed lines mark the position of the Si layers.

calculate the average adsorption induced dipole charge $Q^{\pm}$ and the dipole length projected onto the surface normal, d_z,[30]

$$Q^{\pm} = \int_{\Delta\rho(\mathbf{r})\gtrless 0} d\mathbf{r}\Delta\rho(\mathbf{r}) \tag{4}$$

$$d_z = \frac{1}{Q^{+}}\int_{\Delta\rho(\mathbf{r})>0} d\mathbf{r}\Delta\rho(\mathbf{r})z - \frac{1}{Q^{-}}\int_{\Delta\rho(\mathbf{r})<0} d\mathbf{r}\Delta\rho(\mathbf{r})z. \tag{5}$$

In order to determine the charge transfered parallel to the surface normal, $Q^{\pm}_{||}$, and its separation $d_{||}$, we start from the charge difference averaged over the surface unit cell

$$\overline{\Delta\rho}(z) = \frac{1}{A}\int_{A} dxdy\Delta\rho(\mathbf{r}), \tag{6}$$

and proceed in analogy to Eqs. 4 and 5.

The calculated values for these quantities are compiled in Tab. 1. Obviously, the overall uracil induced charge transfer is rather large, with $Q^{\pm}$ values of 10 – 15 electrons. This is simply due to the substantial rebonding processes taking place upon molecule adsorption. In particular for the models C-2 and D-2 already about 50% of the charge transfer is due to the breaking of Si dimers. Only between 2 – 5 electrons are transferred parallel to the surface normal, with a charge separation between 1.4 – 2.4 Å (cf. Tab. 1). The electrons forming the bonds between uracil and the substrate originate from the substrate rather than from the molecule. There is even some accumulation of additional charge at the adsorbed molecule, as can be seen in Fig. 4. This is plausible, giving the high electronegativity of carbon (2.55), nitrogen (3.04) and oxygen (3.44) compared to the one of silicon (1.9). However, the net electron transfer from the substrate towards the molecule seemingly contradicts the calculated decrease of the ionization energy by up to 2.6 eV. Rather, an increase of the ionization energy would be expected, such as for example found usually upon chlorine adsorption on semiconductor surfaces[31]. The apparent contradiction is due to the dipole moments of the uracil molecules themselves, that form the outermost layer of

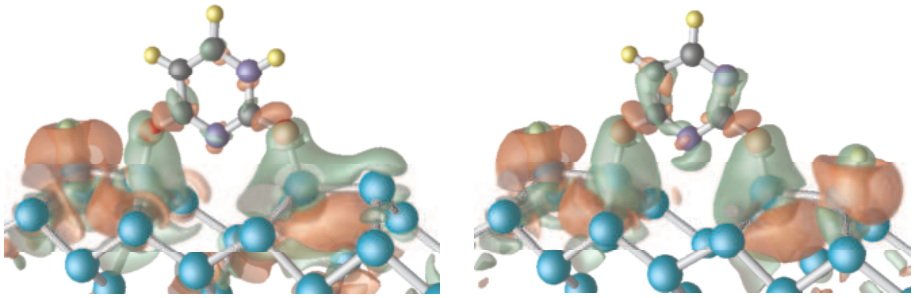

Figure 4. Calculated electron density differences $\Delta\rho(\mathbf{r})$ for the D-1 and C-1 model. Green and orange isosurfaces indicate electron accumulation and depletion regions of $\Delta\rho = \pm 0.03$ Å^{-3}.

the adsorbate system. The uracil dipole moment depends strongly on the specific tautomer. For gas-phase molecules it is up to 7.5 Debye[32]. The molecular dipole points away from the carbonyl groups, thus along the surface normal in the adsorption configurations studied here. Obviously, the ionization energy of organically modified semiconductors depends in a complex way on the nature of the chemical bonds between the organic molecule and the substrate, the closely related molecule-induced charge transfer across the interface as well as the molecular dipole itself.

	d_z	$d_{\|\|}$	$\|Q^{\pm}\|$	$\|Q^{\pm}_{\|\|}\|$	$p_z = \|Q^{\pm}\| \times d_z$	$\overline{\Delta V_C}(z)$
D-1	-0.6	-2.4	9.5	2.5	-29.3	2.6
D-2	-0.7	-2.2	11.7	3.9	-40.8	2.3
C-1	-0.4	-1.4	9.5	2.5	-17.0	0.2
C-2	-0.5	-1.5	15.2	4.9	-35.9	0.5

Table 1. Dipole lengths d_z and $d_{||}$ (in Å), dipole charges $Q^{\pm}$ and $Q^{\pm}_{||}$ (in e), dipole moment p_z (in Debye), and changes of the averaged and smoothed electrostatic Si(001) surface potential due to uracil adsorption (in eV).

4.3 Surface Optical Properties

As shown above, the physical and chemical properties of hybrid organic/inorganic materials depend crucially on the structural and chemical details of the interface. Optical spectroscopies such as reflectance anisotropy spectroscopy (RAS) have been shown to be highly successful in the determination of semiconductor surface structures, see, e.g. Refs. 33, 34. This holds in particular if the measurements are accompanied by accurate *first-principles* calculations[35,36]. We calculate RAS spectra for the uracil/Si(001) bonding geometries shown in Fig. 1 in order to assist in the experimental identification of the actual interface geometries.

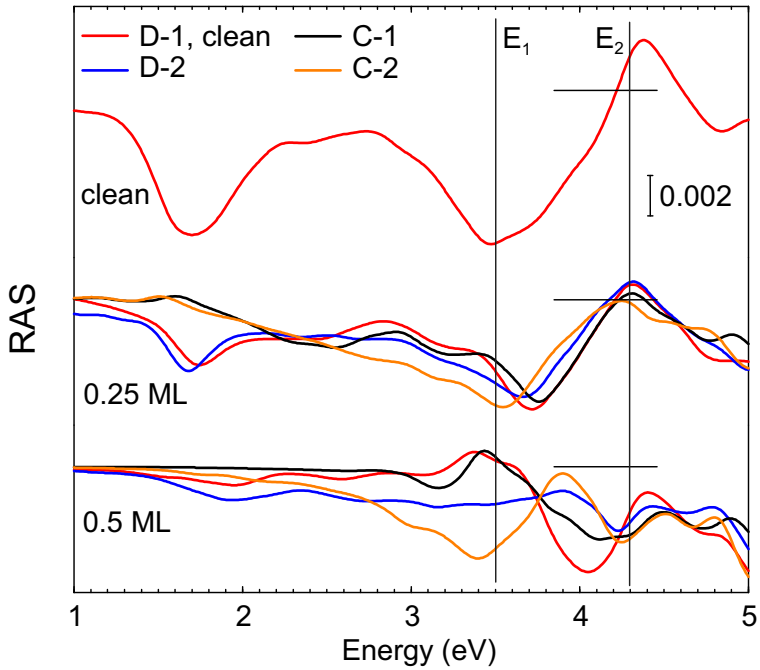

Figure 5. RAS spectra $[Re\{(r_{[\bar{1}10]} - r_{[110]})/ < r >\}]$ calculated for the uracil/Si(001) adsorption configurations shown in Fig. 1 are compared with results for the clean surface. Thin lines are used to indicate the calculated positions of the E_1 and E_2 critical point energies as well as the positions of zero optical anisotropy.

The spectrum calculated for the clean, $c(4\times2)$ reconstructed Si(001) surface is shown in upper part of Fig. 5. It is in excellent agreement with data measured on highly oriented, single-domain Si(001) surfaces prepared by electro-migration[37]. The spectrum changes upon adsorption of uracil. A coverage of 0.25 ML, defined here to correspond to one adsorbed molecule per (4×2) surface unit cell, leads to a complete cancellation or a reduction by a factor of two of the 1.7 eV RAS feature for the covalently or partially dative-bonded adsorption geometries, respectively. This is to be expected. Covalently and dative-bonded interface geometries lead to complete or partial removal of Si-dimer related surface states from the energy region of the fundamental gap.

The modification of the Si(001) RAS signal increases with increasing uracil coverage. For the half-monolayer case all Si surface atoms of the C-1 and C-2 models are covalently bonded. Accordingly, these models show only very weak optical anisotropies below the onset of the bulk transitions at the E_1 critical point energy of Si. In case of D-1 and D-2, one Si surface dangling bond per (4×2) unit cell remains and there is a very weak RAS feature at 1.7 eV. The RAS features between about 3.0 and 4.5 eV are very structure dependent. A sign reversal compared to the clean Si(001) surface is found for the D-1 and D-2 models: positive and negative anisotropies are predicted for photon energies close to the E_1 and E_2 critical point energies, respectively. A similar behavior has been found experimentally[38] and computationally[39] for the structurally similar monohydride Si(001) surface. The RAS signals for the models D-2 and C-2, where oxygen is inserted into the Si

dimers, differ appreciably from the spectra predicted for D-1 and C-1. D-2 shows nearly no variation of the RAS signal below the E_2 critical point energy and C-2 features negative anisotropies at both E_1 and E_2.

5 Concluding Remarks

Several plausible interface configurations for uracil adsorbed on Si(001) have been calculated from *first-principles*. Among the structures investigated, we find that oxygen insertion into Si surface dimers is energetically most favored. It requires, however, to overcome a considerable energy barrier. For moderate annealing temperatures our calculations predict the formation of a structure where uracil bridges two neighboring Si-dimer rows.

The electronic properties of the uracil/Si(001) interface depend strongly on the details of the chemical bonding and adsorption symmetry. The results obtained for different adsorption configurations of the same molecular species on Si suggest the possibility of tuning surface electronic properties by means of choosing suitable preparation conditions such as temperature or by chemically protecting or activating specific molecular functional groups, thus controlling the molecular bonding and orientation with respect to the substrate.

We predict for low uracil coverage the attenuation of the optical anisotropy of the Si(001) surface. For high coverages, i.e., if every Si dimer is involved in the interface bonding, strongly structure dependent changes of the RAS signal are calculated that may allow for discriminating between different interface bonding scenarios. Our calculations suggest the measurement of the surface optical anisotropy as a complementary tool to explore the structural details of organic/inorganic interfaces.

Acknowledgments

Grants of computer time from the John von Neumann-Institut Jülich are gratefully acknowledged. We thank the Deutsche Forschungsgemeinschaft for financial support (SCHM-1361/6).

References

1. K. Seino, W. G. Schmidt, J. Furthmüller, and F. Bechstedt. *Phys. Rev. B*, 66:235323, 2002.
2. W. Lu, W. G. Schmidt, and J. Bernholc. *Phys. Rev. B*, in press.
3. M. Preuss, W. G. Schmidt, K. Seino, and F. Bechstedt. *Appl. Surf. Sci.*, in preparation.
4. K. Seino, W. G. Schmidt, M. Preuß, and F. Bechstedt. *J. Phys. Chem. B*, 107:5031, 2003.
5. J. Dabrowski and H.-J. Müssig. World Scientific, Singapore, 2000.
6. R. J. Hamers, J. S. Hovis, S. Lee, H. Liu, and J. Shan. *J. Phys. Chem. B*, 101:1489, 1997.
7. J. S. Hovis, S. Lee, H. Liu, and R. J. Hamers. *J. Vac. Sci. Technol. B*, 15:1153, 1997.
8. J. S. Hovis, H. Liu, and R. J. Hamers. *Appl. Phys. A*, 66:S553, 1998.
9. S. F. Bent. *J. Phys. Chem. B*, 106:2830, 2002.

10. M. H. Qiao, Y. Cao, J. F. Deng, and G. Q. Xu. *Chem. Phys. Lett.*, 325:508, 2000.
11. X. Cao, S. K. Coulter, M. D. Ellison, H. Liu, J. Liu, and R. J. Hamers. *J. Phys. Chem. B*, 105:3759, 2001.
12. H. Luo and M. C. Lin. *Chem. Phys. Lett.*, 343:219, 2001.
13. J. L. Armstrong, J. M. White, and M. Langell. *J. Vac. Sci. Technol. A*, 15:1146, 1997.
14. J. A. Barriocanal and D. J. Doren. *J. Am. Chem. Soc.*, 123:7340, 2001.
15. G. T. Wang, C. Mui, C. B. Musgrave, and S. F. Bent. *J. Phys. Chem. B*, 105:12559, 2001.
16. G. T. Wang, C. Mui, C. B. Musgrave, and S. F. Bent. *J. Am. Chem. Soc.*, 124:8990, 2002.
17. A. Lopez, Q. Chen, and N. V. Richardson. *Surf. Interface Anal.*, 33:441, 2002.
18. G. Kresse and J. Furthmüller. *Comp. Mat. Sci.*, 6:15, 1996.
19. J. P. Perdew, J. A. Chevary, S. H. Vosko, K. A. Jackson, M. R. Pederson, D. J. Singh, and C. Fiolhais. *Phys. Rev. B*, 46:6671, 1992.
20. D. Vanderbilt. *Phys. Rev. B*, 41:7892, 1990.
21. J. Furthmüller, P. Käckell, F. Bechstedt, and G. Kresse. *Phys. Rev. B*, 61:4576, 2000.
22. M. Preuß, W. G. Schmidt, K. Seino, J. Furthmüller, and F. Bechstedt. *J. Comp. Chem.*, accepted.
23. P. Pulay. *Chem. Phys. Lett.*, 73:393, 1980.
24. D. M. Wood and A. Zunger. *J. Phys. A*, 18:1343, 1985.
25. B. Adolph, J. Furthmüller, and F. Bechstedt. *Phys. Rev. B*, 63:125108, 2001.
26. R. Del Sole. *Solid State Commun.*, 37:537, 1981.
27. F. Manghi, R. Del Sole, A. Selloni, and E. Molinari. *Phys. Rev. B*, 41:9935, 1990.
28. F. Bechstedt. *Festköperprobleme / Advances in Solid State Physics*, volume 32, page 161. Vieweg, Braunschweig/Wiesbaden, 1992.
29. W. G. Schmidt, F. Bechstedt, and G. P. Srivastava. *Surf. Sci. Rep.*, 25:141, 1996.
30. C. Hogan, D. Paget, Y. Garreau, M. Sauvage, G. Onida, L. Reining, P. Chiaradia, and Corradini. *Phys. Rev. B*, submitted.
31. W. Mönch. *Semiconductor Surfaces and Interfaces*. Springer-Verlag, Berlin, 1995.
32. S. X. Tian, C. F. Zhang, Z. J. Zhang, X. J. Chen, and K. Z. Xu. *Chem. Phys.*, 242:217, 1999.
33. D. E. Aspnes. *Solid State Commun.*, 101:85, 1997.
34. W. Richter and J. T. Zettler. *Appl. Surf. Sci.*, 101:465, 1996.
35. W. Lu, W. G. Schmidt, E. L. Briggs, and J. Bernholc. *Phys. Rev. Lett.*, 85:4381, 2000.
36. W. G. Schmidt, P. H. Hahn, F. Bechstedt, N. Esser, P. Vogt, A. Wange, and W. Richter. *Phys. Rev. Lett.*, 90:126101, 2003.
37. R. Shioda and J. van der Weide. *Phys. Rev. B*, 57:R6823, 1998.
38. R. Shioda and J. van der Weide. *Appl. Surf. Sci.*, 130-132:266, 1998.
39. W. G. Schmidt, S. Glutsch, P. H. Hahn, and F. Bechstedt. *Phys. Rev. B*, 67:085307, 2003.